THE ASTROPHYSICAL JOURNAL, 533:L29–L32, 2000 April 10

CHANDRA OBSERVATIONS OF THE CRAB-LIKE SUPERNOVA REMNANT G21.5−0.9

PATRICK SLANE,[1] YANG CHEN,[1,2] NORBERT S. SCHULZ,[3] FREDERICK D. SEWARD,[1]
JOHN P. HUGHES,[4,5] AND BRYAN M. GAENSLER[3,6]

Received 2000 January 28; accepted 2000 February 22; published 2000 March 10

ABSTRACT

Chandra observations of the Crab-like supernova remnant G21.5−0.9 reveal a compact central core and spectral variations indicative of synchrotron burn-off of higher energy electrons in the inner nebula. The central core is slightly extended, perhaps indicating the presence of an inner wind-shock nebula surrounding the pulsar. No pulsations are observed from the central region, yielding an upper limit of ∼40% for the pulsed fraction. A faint outer shell may be the first evidence of the expanding ejecta and blast wave formed in the initial explosion, indicating a composite nature for G21.5−0.9.

Subject headings: ISM: individual (G21.5−0.9) — supernova remnants — X-rays: ISM

1. INTRODUCTION

Supernova remnants (SNRs) in the "Crab-like" or "plerionic" class (Weiler & Panagia 1978) are characterized by compact, filled-center radio morphology, with relatively flat spectral index ($\alpha_r \approx 0.0$–0.3, where $S_\nu \propto \nu^{-\alpha_r}$). The common interpretation is that these remnants are pulsar powered, although direct evidence of an associated pulsar is often lacking. Roughly 5% of the currently cataloged Galactic SNRs (Green 1998)[7] are included in this class, with another 7%–10% classified as "composite" remnants showing plerionic cores accompanied by shells with steeper radio indices ($\alpha_r \approx 0.4$–0.7). The shell-like component is associated with the supernova blast wave and ejecta. In X-rays, the plerionic remnants show nonthermal spectra characteristic of synchrotron emission, while the shell components typically display line-dominated thermal emission, although the shell-type SNRs SN 1006 and G347.3−0.5 are dominated by nonthermal X-rays (Koyama et al. 1995, 1997; Slane et al. 1999).

The absence of any shell or halo of fast-moving ejecta in the Crab Nebula, 3C 58, and other plerionic remnants may be simply the result of a low ambient density which precludes the formation of a detectable shock. Evidence of H I voids around some filled-center remnants (Wallace, Landecker, & Taylor 1994) lends support to this hypothesis, although results for G21.5−0.9 in particular are inconclusive. However, G74.9+1.2 and G63.7+1.1 are filled-center SNRs that show no evidence of fast-moving halos of ejecta, but which appear to be interacting directly with surrounding material (Wallace et al. 1997b; Wallace, Landecker, & Taylor 1997a). Such an interpretation, if correct, could suggest some neutron stars form from underenergetic explosions in which very little material is ejected. Further searches for evidence of extended shell/halo components in Crab-like remnants is thus of considerable importance.

G21.5−0.9 is a compact SNR that exhibits strong linear polarization and centrally peaked emission in the radio band (Morsi & Reich 1987). The radio spectral index is $\alpha_r \sim 0$ for $\nu < 32$ GHz, which puts it in the class of Crab-like SNRs. A steepening of the spectrum is observed beyond 32 GHz (Salter et al. 1989). Previous X-ray observations reveal a similar morphology (Becker & Szymkowiak 1981) with a hard X-ray spectrum (Asaoka & Koyama 1990). To date, there has been no detection of a central pulsar (Frail & Moffett 1993; Kaspi et al. 1996).

Neutral hydrogen absorption measurements place G21.5−0.9 at a distance of ∼4.8 kpc (Becker & Szymkowiak 1981). Throughout this Letter we assume $d = 5$ kpc and show the scaling of relevant quantities with $d = 5d_5$ kpc explicitly.

The radio luminosity of G21.5−0.9 is $1.8 \times 10^{34} d_5^2$ ergs s^{-1} ($\nu < 32$ GHz; Morsi & Reich 1987), and it has a lower L_X/L_r ratio than the Crab; it is a factor of ∼9 less luminous in the radio and a factor of ∼100 less in X-rays. Previous measurements fail to show evidence of any extended component outside the plerion.

2. OBSERVATIONS AND ANALYSIS

G21.5−0.9 has been observed regularly as a calibration target for the *Chandra X-Ray Observatory* (Weisskopf, O'Dell, & van Speybroeck 1996). Here we concentrate on an early set of observations carried out on 1999 August 23 and October 25. We select Advanced CCD Imaging Spectrometer (ACIS) observations with the remnant placed on the S3 chip, where the best focus is achieved, and use these for both spectral and spatial information. We use observations with the High-Resolution Camera (HRC) to obtain the highest angular (∼0.″5) and time resolution information. The observations used for this study are summarized in Table 1.

In Figure 1 (*left*) we present the HRC image of the plerion. At the center of the X-ray image is a bright compact region which contains ∼8% of the total flux. This central emission is extended beyond the ∼0.″5 resolution of the telescope, however. A comparison of the emission profile with that for a point source at the same on-axis position in the HRC reveals an extent of ∼2″ (Fig. 1), corresponding to a source size of $\sim 0.05 d_5$ pc. An investigation of timing data from the central region yields no significant evidence for pulsations; we derive an upper limit of ∼40% for the pulsed fraction in the HRC bandpass (∼0.1–10 keV) assuming a sinusoidal light curve.

[1] Harvard-Smithsonian Center for Astrophysics, 60 Garden Street, Cambridge, MA 02138.
[2] Department of Astronomy, Nanjing University, Nanjing 210093, P. R. China.
[3] Center for Space Research, Massachusetts Institute of Technology, Cambridge, MA 02139.
[4] Department of Physics and Astronomy, Rutgers, State University of New Jersey, Piscataway, NJ 08854-8019.
[5] Service d'Astrophysique, L'Orme des Merisiers, CEA-Saclay, 91191 Gif-sur-Yvette Cedex, France.
[6] Hubble Fellow.
[7] Available at http://www.mrao.cam.ac.uk/surveys/snrs.

TABLE 1
SUMMARY OF OBSERVATIONS

Observation	Instrument	Duration (ks)	Date (1999)
159	ACIS (S3)	17.7	23 Aug
1230	ACIS (S3)	15.8	23 Aug
1406	HRC-I	30	25 Oct

The next largest structure is the main body of the plerion, which has a radius of roughly 30″, with some variation in size—particularly in the northwestern region, which shows a distinct indentation. The ACIS data for the plerion reveals a nonthermal spectrum with energy index $\alpha_X \sim 0.9$ and a column density $N_H \sim 2 \times 10^{22}$ cm^{-2}. The latter is consistent with the H I absorption measurements (Davelaar, Smith, & Becker 1986). Here we have used a radius of 40″ to extract events from the entire plerion; background was taken from regions of the same detector well separated from the remnant. For comparison, we have used *ASCA* data to fit the spectrum and find excellent agreement with the values derived from the *Chandra* data.

The X-ray luminosity of the plerion is $L_X = 2.1 \times 10^{35} d_5^2$ ergs s^{-1}. When the column density is fixed at the value above, we find that the spectral index varies with radius, as indicated in Figure 2. This spectral softening with increasing radius, which is also observed for 3C 58 (Torii et al. 2000), is consistent with synchrotron burn-off of electrons accelerated in the central regions; due to the short synchrotron lifetime for higher energy electrons, only the lower energy component is able to survive to the outer regions of the plerion. The spectral index of the compact core is $\alpha_X = 0.5$, similar to that of the Crab pulsar.

Perhaps the most interesting result from the ACIS observations is the presence of a very faint outer shell or halo in G21.5−0.9. As illustrated in Figure 1 (*right*), the shell radius is roughly 1.′2–2′, corresponding (1.7–2.9) d_5 pc. The faint shell is incomplete in the southwest and shows several knots in the northern region. The spectrum of this outer region is difficult to quantify at this early stage of the *Chandra* calibration efforts. Using data with a combined integration time of 33.5 ks, we obtained four spectra with a total of ~8700 counts; these spectra were fit simultaneously. Combining data from observations with different CCD chips is, at this stage, not possible. The spectrum, which is relatively hard, can be adequately described by either a power law or an optically thin thermal spectrum (e.g., Raymond & Smith 1977). The results are listed in Table 2.

3. DISCUSSION

The nonthermal nature of the X-ray emission from the core of G21.5−0.9 indicates the presence of a central pulsar that powers the synchrotron nebula. X-ray studies of pulsars indicate a correlation between the total nonthermal X-ray luminosity of the systems and the spin-down power $\dot{E}$ of the pulsar (e.g., Seward & Wang 1988; Becker & Trümper 1997). Our best fit for this relation gives $L_X = 3 \times 10^{-11} \dot{E}^{1.22}$, where we have used 0.1–2.4 keV luminosity values. Using the luminosity in Table 2, we infer the presence of a pulsar with $\dot{E} = 3.5 \times 10^{37} d_5^{1.6}$ ergs s^{-1}. This is large for the general pulsar population, but reasonable for a young pulsar associated with a synchrotron nebula.

Applying standard synchrotron emission calculations (Ginzburg & Syrovatskii 1965) to the radio spectrum from G21.5−0.9, under the assumption of a power-law electron distribution (see Harrus, Hughes, & Slane 1998), we derive a nebular magnetic field $B = 4.4 \times 10^{-4} d_5^{-2/7} \theta_{30}^{-6/7}$ G and a magnetic pressure $P_B = 7.7 \times 10^{-9} d_5^{-4/7} \theta_{30}^{-12/7}$ dyn cm^{-2}.

Balancing the ram pressure of a pulsar-driven wind ($\dot{E}/4\pi\eta c r_w^2$, where the wind covers a fraction η of a sphere) with the nebular magnetic pressure, we estimate a termination shock radius $r_w \approx 0.04 \eta^{-1/2} d_5^{1.1} \theta_{30}^{6/7}$ pc. This corresponds to an angular size of $\sim 1.''5 \eta^{-1/2}$ for the distance and nebular size estimates used above. Interestingly, this is consistent with the apparent extent of the central source in G21.5−0.9 (Fig. 1). It may be that the pulsar itself is hidden from our view beneath the shroud of the termination shock. For the Crab pulsar, radio observations reveal filamentary "wisps" (Bietenholz & Kronberg 1992) thought to be produced at this boundary zone in which the pulsar wind begins decelerating through interactions with the surrounding medium (Rees & Gunn 1974). Similar evidence of a radio wisp is observed in 3C 58 (Frail & Moffett

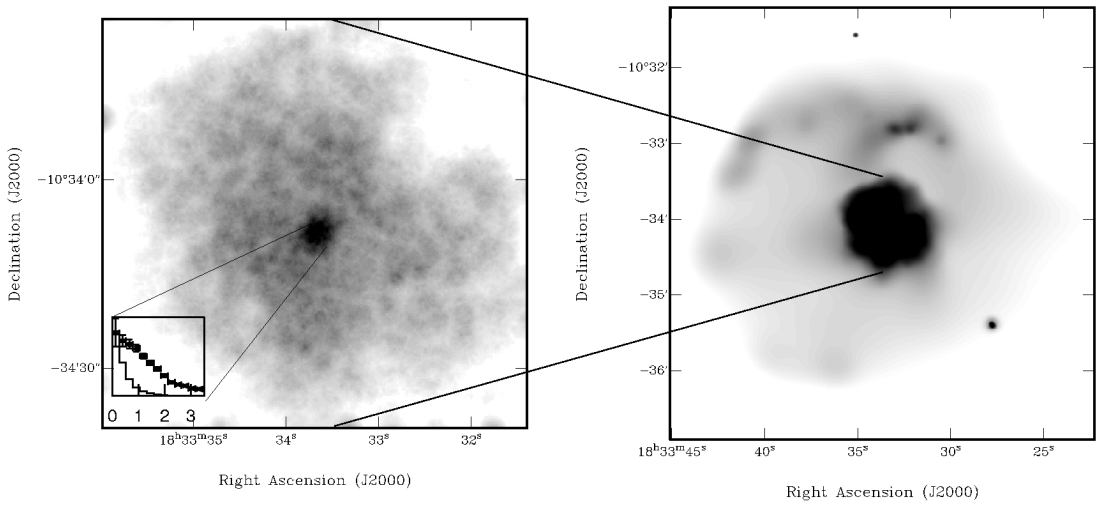

FIG. 1.—*Left:* HRC image of the plerionic component of G21.5−0.9. The image has been adaptively smoothed with a Gaussian whose width varies inversely with the number of counts in the image. The inset shows the brightness profile of the center (*points*) compared with that for a point source (*histogram*). Intensity units are arbitrary, and units on horizontal scale are arcseconds. *Right:* ACIS image of G21.5−0.9 revealing faint halo of emission surrounding the synchrotron core. The image has been adaptively smoothed in a manner similar to that used for the HRC image. The bright source is positionally coincident with the emission-line star SS 397.

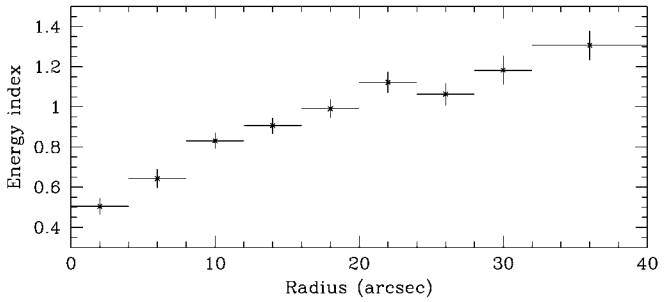

FIG. 2.—Variation of power-law index with radius for the synchrotron core of G21.5−0.9.

1993), and the separation of the feature from the compact X-ray source observed in this SNR (Helfand, Becker, & White 1995) appears compatible with calculations of the expected termination shock distance (Torii et al. 2000).

The extrapolation of the X-ray spectrum of the plerion as a whole to IR frequencies is inconsistent with the measured *ISO* flux (Gallant & Tuffs 1998); the measured IR flux exceeds the prediction. This curious result may result from oversimplification of the X-ray spectrum, however. As shown in Figure 2, the spectral index increases with radius. A value of $\alpha_X \sim 1.0$, compatible with the outer regions of the nebula, provides good agreement upon extrapolation to the IR band. Alternatively, this may be indicative of the time evolution of the energy input into the nebula from the central source. We note that the X-ray core has no observed counterpart in the radio or IR bands.

The faint, extended halo of emission from G21.5−0.9 presumably represents the contribution from the SNR ejecta, with the brighter clumps in the northwest being associated with regions in which the ejecta have encountered material of higher density. Faint arcs discernible in Figure 1 could be indicative of a reverse shock being driven into the expanding ejecta. Alternatively, the X-ray emission from the diffuse halo could be dominated by synchrotron emission from relativistic electrons accelerated at the shock front as proposed for SN 1006 and G347.3−0.5.

The presence of an extended X-ray halo surrounding the Crab-like core of G21.5−0.9 raises the question of whether there is also an extended radio halo corresponding to the shell morphology seen in the vast majority of radio SNRs. We have examined archival Very Large Array data and find no radio shell around G21.5−0.9 down to a 1 GHz surface brightness limit (1 σ) of $\Sigma = 4 \times 10^{-21}$ W m^{-2} Hz^{-1} sr^{-1}. While this is sufficient to detect most young SNRs, at least one Crab-like source (G322.5−0.1) has a shell component that would not be seen down to this limit (Whiteoak 1992).

If the extended halo truly represents the fast-moving ejecta, we would expect the spectrum to reveal characteristic emission-line features from the hot gas. As summarized in Table 2, the best-fit spectrum is an absorbed power law. While we present results with the column density fixed to that obtained for the plerion, we note that slightly better spectral fits are obtained for a somewhat lower value of 1.8×10^{22} cm^{-2}. A model for thermal emission (Raymond & Smith 1977) provides an adequate fit (although inferior to the power law) with a temperature of 2.8 keV. Based upon the thermal model, the mean density of the emitting material is $n_H = 1.1\phi_{1.5}^{-3/2} d_5^{-1/2} f^{-1/2}$ cm^{-3}, where $\phi_{1.5}$ is the angular radius of the shell in units of 1.′5 and f is the fraction of the spherical volume comprising the X-ray emission. The mass of the emitting material is then $M_X = 1.2\phi_{1.5}^{3/2} d_5^{5/2} f^{1/2}\ M_\odot$. With such a small amount of swept up material, G21.5−0.9 is still dynamically young.

If the extended emission is nonthermal, then G21.5−0.9 joins SN 1006 and G347.3−0.5 as remnants whose shell emission is dominated by nonthermal processes in X-rays. The absence of an observed radio shell is consistent with the low radio surface brightness of these other remnants. More importantly, since the plerionic core in G21.5−0.9 implies a massive progenitor, while SN 1006 is the result of a Type Ia explosion, the addition of G21.5−0.9 to this class would imply that the nonthermal X-ray shells are related more to environment than to progenitor type.

4. CONCLUSIONS

The early *Chandra* observations of G21.5−0.9 have revealed new information on all spatial scales. The variation in spectral index with radius in the plerion supports the view that a central object injects energetic electrons into the surrounding region and that the lower energy particles, whose synchrotron radiation lifetimes are longest, predominate at the outskirts of the nebula. The center of the plerion shows a compact core which presumably contains a neutron star that powers the system, but this core is not pointlike; an extended shroud, possibly associated with the pulsar wind termination shock, apparently hides the pulsar itself. No pulsations are detected from the central region.

On the largest scales, a faint halo of emission is observed, with some evidence of arcs and clumplike features. This may correspond to the contribution from the fast-moving ejecta, although the spectral information is too sparse to quantify the nature of the emission in detail. If this component does indeed correspond to the ejecta component, then G21.5−0.9 does not fall into the proposed category of low explosion energy remnants with no ejecta proposed as possible progenitors to the class of plerionic SNRs. Deeper observations of the remnant are needed to better constrain this extended component. Upcoming studies with *XMM* have an excellent chance of clarifying this situation.

This work was supported in part by the National Aeronautics and Space Administration through contract NAS8-39073 (P. S.) and grant NAG5-6420 (J. P. H). Y. C. acknowledges support from the Huaying Cultural and Educational Founda-

TABLE 2
G21.5−0.9 SPECTRAL FITS

Region	N_H ($\times 10^{22}$ cm^{-2})	α_X (energy)	kT (keV)	F_x (ergs cm^{-2} s^{-1})[a]	χ^2 (dof)
Plerion[b]	2.24 ± 0.04	0.91 ± 0.04	…	7.0×10^{-11}	2171 (1671)
Shell:					
Thermal	2.24 (fixed)	…	2.8 ± 0.2	8.4×10^{-12}	520 (369)
Nonthermal	2.24 (fixed)	1.56 ± 0.05	…	1.2×10^{-11}	379 (369)

[a] Unabsorbed flux (0.5–10 keV).
[b] Entire synchrotron nebula.

tion. B. M. G. acknowledges the support of NASA through Hubble Fellowship grant HF-01107.01-98A awarded by STScI, which is operated by AURA, Inc., for NASA under contract NAS5-26555.

REFERENCES

Asaoka, I., & Koyama, K. 1990, PASJ, 42, 625
Becker, R. H., & Szymkowiak, A. E. 1981, ApJ, 248, L23
Becker, W., & Trümper, J. 1997, A&A, 326, 682
Bietenholz, M. F., & Kronberg, P. P. 1992, ApJ, 393, 206
Davelaar, J., Smith, A., & Becker, R. H. 1986, ApJ, 300, L59
Frail, D. A., & Moffett, D. A. 1993, ApJ, 408, 637
Gallant, Y. A., & Tuffs, R. J. 1998, Mem. Soc. Astron. Italiana, 69, 963
Ginzburg, B. L., & Syrovatskii, S. I. 1965, ARA&A, 3, 297
Green, D. A. 1998, A Catalogue of Galactic Supernova Remnants (1998 September version; Cambridge: MRAO)
Harrus, I. M., Hughes, J. P., & Slane, P. O. 1998, ApJ, 499, 273
Helfand, D. J., Becker, R. H., & White, R. L. 1995, ApJ, 453, 741
Kaspi, V. M., Manchester, R. N., Johnston, S., Lyne, A. G., & D'Amico, N. 1996, AJ, 111, 2028
Koyama, K., Kinugasa, K., Matsuzaki, K., Nishiuchi, M., Sugizaki, M., Torii, K., Yamauchi, S., & Aschenbach, B. 1997, PASJ, 49, L7
Koyama, K., Petre, R., Gotthelf, E. V., Hwang, U., Matsura, M., Ozaki, M., & Holt, S. S. 1995, Nature, 378, 255
Morsi, H. W., & Reich, W. 1987, A&AS, 69, 533
Raymond, J. C., & Smith, B. 1977, ApJS, 35, 419
Rees, M. J., & Gunn, R. E. 1974, MNRAS, 167, 1
Salter, C. J., Reynolds, S. P., Hogg, D. E., Payne, J. M., & Rhodes, P. J. 1989, ApJ, 338, 171
Seward, F. D., & Wang, Z.-R. 1988, ApJ, 332, 199
Slane, P., Gaensler, B. M., Dame, T. M., Hughes, J. P., Plucinsky, P. P., & Green, A. 1999, ApJ, 525, 357
Torii, K., Kinugasa, K., Hashimotodani, K., Tsunemi, H., & Slane, P. 2000, PASJ, submitted
Wallace, B. J., Landecker, T. L., & Taylor, A. R. 1994, A&A, 286, 565
———. 1997a, AJ, 114, 2068
Wallace, B. J., Landecker, T. L., Taylor, A. R., & Pineault, S. 1997b, A&A, 317, 212
Weiler, K. W., & Panagia, N. 1978, A&A, 70, 419
Weisskopf, M. C., O'Dell, S. L., & van Speybroeck, L. P. 1996, Proc. SPIE, 2805, 2
Whiteoak, J. B. Z. 1992, MNRAS, 256, 121